Macromolecules

ARTICLE

pubs.acs.org/Macromolecules

Microphase-Separated Structures of Poly(4-*tert*-butylstyrene-*block*-4-*tert*-butoxystyrene) upon Gradual Changes in Segregation Strength through Hydrolysis Reaction

Siti Sarah Abdul Rahman, Daisuke Kawaguchi, and Yushu Matsushita*

Department of Applied Chemistry, Graduate School of Engineering, Nagoya University, Furo-cho, Chikusa-ku, Nagoya 464-8603, Japan

ABSTRACT: The morphological change of poly(4-*tert*-butylstyrene-*block*-4-*tert*-butoxystyrene)s (BO) upon hydrolysis reaction was investigated by transmission electron microscopy (TEM) and small-angle X-ray scattering (SAXS). Poly(4-*tert*-butoxystyrene) (O) can be converted into poly(4-hydroxystyrene) (H) through hydrolysis reaction. Four BOs having number-average molecular weight, M_n, from 38K to 148K were synthesized, and copolymers with various conversion rates of O into H, f_Hs, were prepared. No microphase-separated structure is observed for nonhydrolyzed samples, while all hydrolyzed ones exhibit predominantly lamellar structures with a small portion of cylindrical one. These results indicate that the repulsive force between blocks becomes stronger upon hydrolysis reaction. Domain spacing of the lamellar structure, D, is found to increase with an increase in f_H, where it abruptly increases at a critical conversion rate, $f_{H,c}$, indicating that the chains stretched perpendicularly to the lamellar interface. The normalized domain spacings, D/D_0, where D_0 is the correlation length at $f_H = 0$, were scaled by segregation strength, χN, where χ is the interaction parameter and N is the degree of polymerization. Three regimes can be distinguished in the plot of D/D_0 vs χN: (I) the weak segregation regime with $D/D_0 \sim 1$ that associates with the scaling behavior of $D \sim N^{0.55}$, (II) the intermediate segregation regime with the scaling behavior of $D/D_0 \sim (\chi N)^{0.34}$, and (III) the strong segregation regime with $D/D_0 \sim 2.3$ which corresponds to $D \sim N^{0.67}$. Rough computation of D based on strong segregation limit theory shows that hydrogen bonding from self-association of H compensates for the repulsive force among components leading to a constant D after $f_{H,c}$.

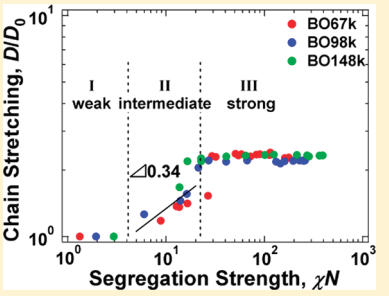

INTRODUCTION

Microphase-separated structures of block copolymers have potentials in applications such as nanoporous materials,[1−6] templates of nanoparticles,[7,8] high-conductivity nanocomposite,[9] and dye-sensitized solar cell,[10] etc. In order to have flexible access in controlling microphase-separated structures, understanding the thermodynamics of block copolymers is crucial. In general, the morphologies of block copolymers are controlled by volume fraction, ϕ, and the degree of segregation, χN, where χ is the interaction parameter and N is the total degree of polymerization. Many reports have elucidated the role of χN by focusing on N. It has been found that the domain spacing of the microphase-separated structure, D, can be scaled with N as $D \sim N^{\delta}$, where $\delta = 1/2$ if the interactions between the components are sufficiently weak that the individual chains are unperturbed (Gaussian statistics).[11−14] This scaling behavior refers to the weak segregation limit (WSL). When χN increases, block copolymers form microphase-separated structures. $D \sim N^{2/3}$ is realized when strong repulsive force acts on the different species in block copolymers, resulting in narrow interface and well-separated microdomains.[15−20] This limiting regime is called strong segregation limit (SSL). Despite WSL and SSL, there are several reports on intermediate segregation limit (ISL) where strong concentration fluctuation near the order−disorder transition (ODT) leads to $\delta = 4/5$, which is larger than the SSL exponent.[21−26] Thus, the phase transition of block copolymers has been investigated in a limited χN region separately. However, the whole feature of the phase transition has not been examined using only one type of block copolymer covering a wide range of χN from WSL to SSL through ISL.

The effect of χ on microphase-separated structures has not been investigated in detail. Even though χ has been empirically shown to be a function of temperature from scattering studies, it is difficult to vary χ in a wide range because the temperature dependence of χ is usually small for polymers.[27] In principle, the study of χ on block copolymer morphology can be conducted by using block copolymers having constant length but different chemical structures. However, this is unrealistic because it is difficult to control N during synthesis and difficult to know the values of χ for many polymer pairs.

χ of a block copolymer can be gradually varied if a component can undergo changes in chemical structure through a chemical reaction, i.e., change the chemical nature of a component. For examples, polydienes, polyesters, and polyamines, etc., are known to undergo chemical modification through hydrolyzation,[28−31] hydrogenation,[31−34] sulfonation,[35,36] and fluorination.[37,38] Some have applied this idea to study the effects of chemical modification on microphase-separated structures of block copolymers.[38−40]

Received: October 26, 2010
Revised: February 23, 2011
Published: March 17, 2011

Table 1. Molecular Characteristics of BOs

sample[a]	M_n	M_w/M_n	$\phi_{B,before}$[b]	$\phi_{B,after}$[c]	N[d]
BO38k	38K	1.05	0.47	0.60	224
BO67k	67K	1.02	0.45	0.58	399
BO98k	98K	1.07	0.51	0.64	583
BO148k	148K	1.04	0.55	0.67	882

[a] Numbers in the sample codes represent M_ns. [b] Volume fraction of B component, ϕ_B, before hydrolysis reaction. [c] ϕ_B after full conversion of O into H. [d] Degree of polymerization, N.

It was found that gyroid structure appears to be stable in SSL in contrast to theoretical predictions for a fluorinated diblock copolymer.[38a] In another study, various morphologies besides lamellar structure were observed for a series of sulfonated block copolymer even though the composition is 1:1.[39] These studies show that chemical modification is a good method to control the morphology of block copolymers.

In this study, we investigate the changes in microphase-separated structures of poly(4-*tert*-butylstyrene-*block*-4-*tert*-butoxystyrene) (BO) upon hydrolysis reaction. Poly(4-*tert*-butoxystyrene) (O) can be easily converted into poly(4-hydroxystyrene) (H) through hydrolysis reaction. Since O is a nonpolar polymer and H is a polar one,[41] the conversion of O into H should sensitively change the segregation strength in the copolymer, thus altering its aggregation state. Moreover, because of the simplicity of hydrolysis reaction where it can be conducted by just adding acid to a polymer solution, segregation power can be tuned gradually and finely. Therefore, we focused on the morphologies of hydrolyzed BOs at various degrees of hydrolysis in order to study the aggregation states of the chains by precisely investigating the $D-N$ relationship.

EXPERIMENTAL SECTION

Sample Preparations. Four symmetric BOs having different molecular weights were prepared by sequential living anionic polymerizations in THF at −78 °C under vacuum using *sec*-BuLi and methanol as an initiator and a terminator, respectively. Number-average molecular weights, M_ns, were determined by membrane osmometry (OSMOMAT-090, Gonotec GmbH), and molecular weight distribution, M_w/M_n, was obtained from gel permeation chromatography (GPC) (HLC-8020, Tosoh Corp.). Volume fractions of B before and after hydrolysis reaction ($\phi_{B,before}$ and $\phi_{B,after}$) were estimated by ^{1}H NMR (Varian INOVA, Varian) based on the mass densities of B, O, and H homopolymers.[41] Since the mass density of H (=1.16 g/cm^3) is much larger than that of O (=1.00 g/cm^3), the $\phi_{B,after}$ values are considerably higher than the corresponding $\phi_{B,before}$ ones. Table 1 represents the molecular characteristics of BOs used in this study. All BOs are abbreviated with their M_ns. Note that the relation between the glass transition temperature of O/H mixed block and f_H slightly deviates from linearity. Thus, volume fraction of hydrolyzed BO may not be necessarily a simple linear combination of the melt densities of the constituents but can be roughly estimated based on f_H.

Hydrolysis Reaction. Hydrolysis reactions were conducted by heating 5 wt % of 1,4-dioxane solutions of BOs under the presence of concentrated hydrochloric acid (HCl). The conversion from O into H, f_H, was controlled by reaction time, temperature, and HCl concentration. f_H was measured by ^{1}H NMR at 500 MHz. To prevent H component from forming aggregation, the samples were dissolved in a mixture of deuterated chloroform ($CDCl_3$) and deuterated dimethyl sulfoxide (DMSO-d_6) at a ratio of 1:1. $CDCl_3$ is a good solvent for B and O, while DMSO-d_6 is a selective solvent for H. The conversion rate for BO67k is shown in Figure 1. The f_H values linearly increase with reaction time, and their values become higher at high temperature and high HCl concentration conditions. Hence, samples having f_H ranging from 0 to 1 were managed to be prepared by controlling the temperature, reaction time, and HCl concentration of hydrolysis reaction.

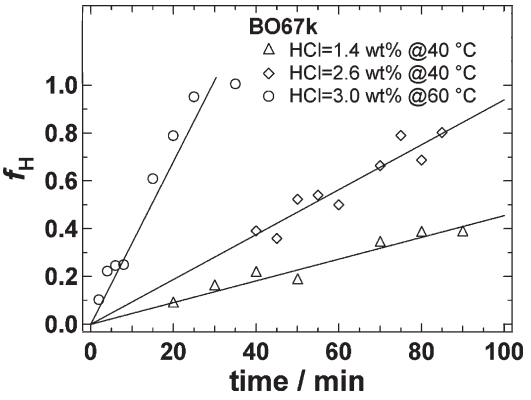

Figure 1. Conversion rate, f_H, of BO67k. Hydrolysis reaction was conducted at three different conditions by varying reaction temperature and HCl concentration.

Morphological Observation. Microphase-separated structures of hydrolyzed BOs were examined by transmission electron microscopy (TEM) and small-angle X-ray scattering (SAXS). Film samples were prepared by casting from their THF solutions. Films were then dried under vacuum at 50 °C for a day to remove remaining solvent and finally annealed at 190 °C, a temperature above the glass transition temperature, T_g, of all components (T_gs of B, O, and H are 103, 145, and 183 °C, respectively) under vacuum for 5 days. Higher temperature was not applied for annealing to prevent samples from degradation. This long annealing time was employed to make up with the only 10 °C difference between annealing temperature and T_g. For TEM observation, films were cut into ultrathin films of 50 nm thickness and stained with ruthenium tetroxide (RuO_4). TEM observation was conducted by using a microscope of Hitachi, model H-7100, and the acceleration voltage was 100 kV. SAXS measurements were carried out at BL15A, Photon Factory, High Energy Accelerator Research Organization, Japan. The camera length was 2.3 m, and the wavelength of the X-ray was 0.15 nm.

RESULTS AND DISCUSSION

Morphologies of Hydrolyzed BOs. Figure 2a shows the TEM images for BO38k series having various f_Hs. Since the samples were stained with RuO_4, B phase appears dark, while O/H mixed phase is bright. No microphase-separated structure was observed for BO38k before hydrolysis reaction, indicating that it is in a disordered state and that the repulsive force between poly(4-*tert*-butylstyrene) (B) and O is weak. However, upon acid treatment, microphase-separated structures were formed. This implies that the repulsive force between B and H blocks is much stronger than that between B and O. For samples having f_H of 0.12, 0.27, 0.32, and 0.40, the coexistence of both lamellar and cylindrical structures was found. On the other hand, only lamellar structure was observed for samples of f_H = 0.71 and 1.00. The formation of lamellar structure in all samples is consistent with the statistical behavior of hydrolysis reaction.[42] Even though ϕ_B increases with f_H, ϕ_Bs are still within the range in which the block copolymers show lamellar structure. Meanwhile, cylindrical structure may be attributed to the localization of the block sequence of H units due to the fluctuation in hydrolysis.[42]

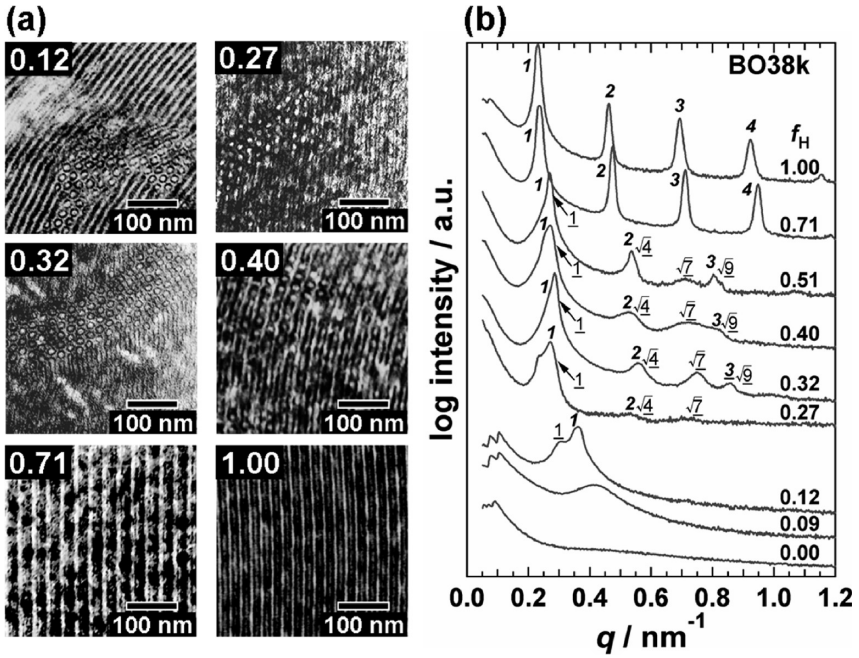

Figure 2. (a) TEM images and (b) SAXS profiles of BO38k series having various f_H values. The numbers at the upper left-hand of each TEM micrograph represent f_H. B phase appears dark, whereas O/H phase is bright. Integer order numbers in SAXS profile indicate lamellar structures, while the underlined square root ones denote cylindrical structures.

Table 2. Values of d_{lam} and d_{cyl} of BO38k

f_H	d_{lam}/nm	d_{cyl}/nm
0.12	10.1	7.5
0.27	10.7	8.1
0.32	11.1	8.5
0.40	11.6	10.4
0.71	13.6	
1.00	13.7	

H-clustered multiblock-like sequence may cause deviations in the interfacial curvature, thus forming isolated cylindrical domains leaving O-rich sequence to exist in B phase. In order to confirm this, the diameters of the cylindrical structures, d_{cyl}s, were estimated based on TEM images and compared with the thickness of O/H domains in the lamellar structures, d_{lam}s. The values of d_{lam} and d_{cyl} for BO38k are tabulated in Table 2. The d_{cyl} values increase with an increase in f_H and are smaller than the d_{lam} value at a given f_H. These results imply that H-rich multiblock-like sequence is formed and that the characteristic length is smaller than the fully hydrolyzed O block. An unusual local structure was seen in samples of $f_H = 0.12$ and 0.32 where the O/H domains are surrounded by rings of B with O/H on the outside. H units are probably distributed between B block and O-rich sequence creating a triblock-like sequence of B-(H-rich)-(O-rich). However, SAXS profiles do not show any scattering peaks from core−shell-like structure. Furthermore, it was found that the fraction of cylindrical structure is roughly ca. 20% based on the area of hexagonally packed domains in low-magnified TEM images, indicating its minor existence.

The corresponding SAXS profiles are displayed in Figure 2b. The BO38k with f_H of 0.00 and 0.09 showed correlation hole peaks around q = 0.43 nm^{-1}. Meanwhile, scattering peaks originated from microphase-separated structures were detected in f_H ranging from 0.12 to 1.00 where high order peaks were detected in all samples except for that of 0.12. Even though clear TEM images were obtained even for f_H of 0.12, the SAXS peak intensity is weak probably due to low degree of orientation of phase-separated domains. Integer order peaks representing lamellar structures were observed in hydrolyzed samples with f_H of 0.27 and higher. The positions of principal peaks shift to lower scattering vector, q (= $(4\pi/\lambda)\sin(\theta/2)$ where λ is the wavelength of the X-ray and θ is the scattering angle), with an increase in f_H, indicating an increase in D as hydrolysis reaction proceeds. In addition, peaks having a series of ratios of peak positions to the primary peak of 1:$\sqrt{4}$:$\sqrt{7}$:$\sqrt{9}$ were recognized in samples with f_H ranging from 0.27 to 0.51, which correspond to cylindrical structures indicating the existence of both lamellar and cylindrical structures in these samples. Hence, the morphologies investigated by SAXS are in good agreement with TEM observations.

The morphologies of the hydrolyzed BO67k, BO98k, and BO148k are represented in Figures 3−5. All nonhydrolyzed BOs were transparent under TEM, and their SAXS profiles showed only correlation hole peaks. These results imply that they are all in disordered states. In contrast, lamellar structures were mainly observed in all the hydrolyzed samples, which were guaranteed by the integer order peaks in the SAXS profiles. We observed nonoriented structures for f_H of 0.05 and 0.11 in BO67k, while the coexistence of lamellar and cylindrical structures was conceived for samples with f_H ranging $0.25 \leq f_H \leq 0.61$. Even though the TEM images for BO98k series and BO148k series only showed lamellar structure, irregularities in the SAXS profiles were observed. The existence of another structure suggested by peaks indicated with arrows in Figures 4b and 5b found in samples of f_H = 0.19, 0.23, and 0.35 of BO98k and f_H = 0.21 and 0.36 of BO148k. The peaks cannot be assigned to a specific

dx.doi.org/10.1021/ma102440a |*Macromolecules* 2011, 44, 2799–2807

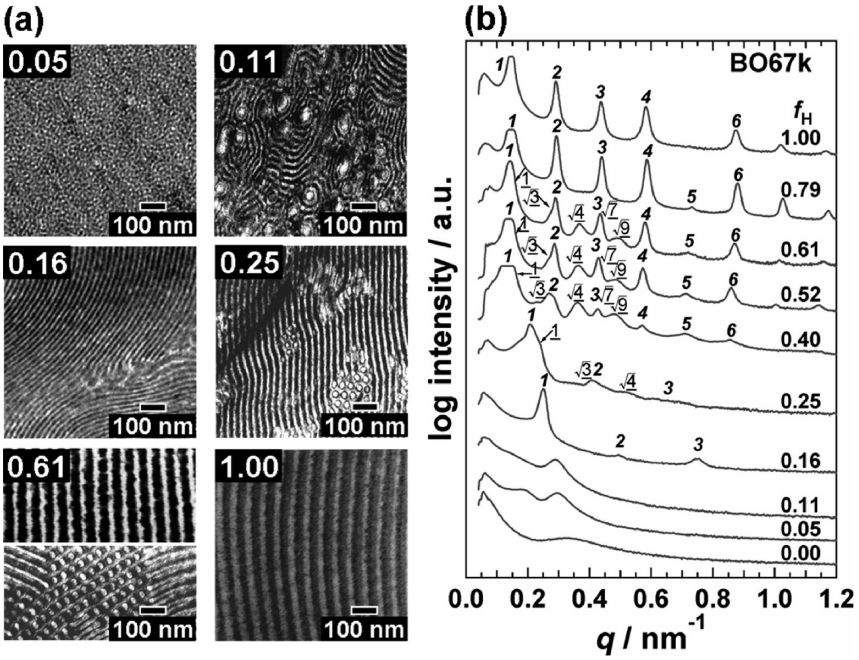

Figure 3. (a) TEM images and (b) SAXS profiles of BO67k having various f_H values. The numbers at the upper left hand of each TEM micrograph represent f_H. Integer order numbers in SAXS profile indicate lamellar structures, while the underlined square root ones denote cylindrical structures.

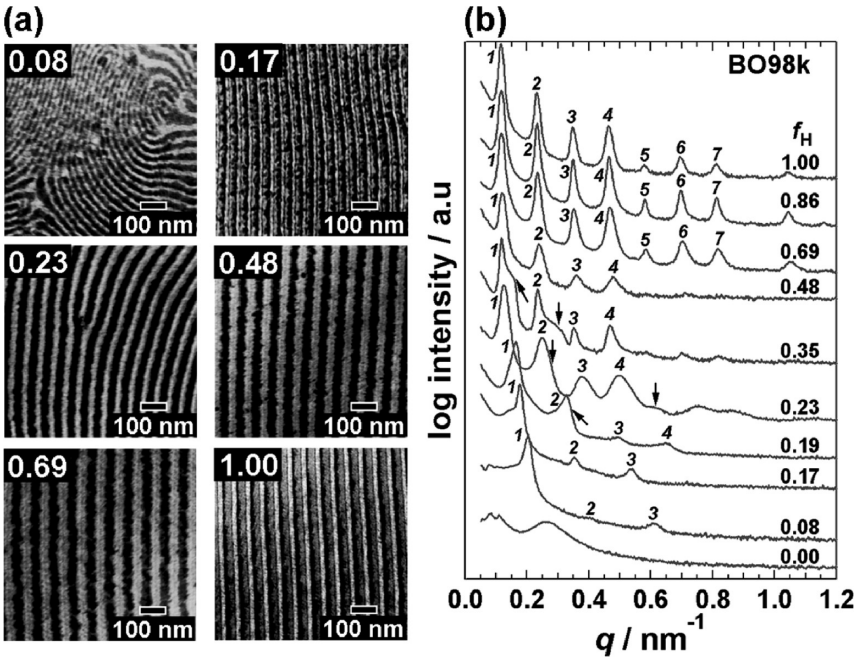

Figure 4. (a) TEM micrographs and (b) SAXS profiles of BO98k having various f_H values. The numbers at the upper left hand of each TEM micrograph represent f_H. Integer order numbers in SAXS profile indicate lamellar structures, while the arrows denote another structure.

structure due to the uncertainty of the primary peaks and the absence of high order peak. Nevertheless, their low intensity implies that they are only formed in a small portion where lamellar structure still remains as the major component. Hence, the changes in morphology are consistent in all BOs upon converting O into H which are due to the increase in the segregation strength.

Changes in Lamellar Domain Spacing upon Hydrolysis Reaction. To examine the effect of χ variation on domain spacing, we focus on the lamellar structure because the statistical behavior of hydrolysis is kept hold. Figure 6 displays the relationship between D and f_H for BO38k, BO67k, BO98k, and BO148k. D was calculated from $2\pi/q_1$, where q_1 is the magnitude of the scattering vector for the primary peak. Ds at $f_H = 0$ were represented by correlation lengths, D_0s, taken from the peak

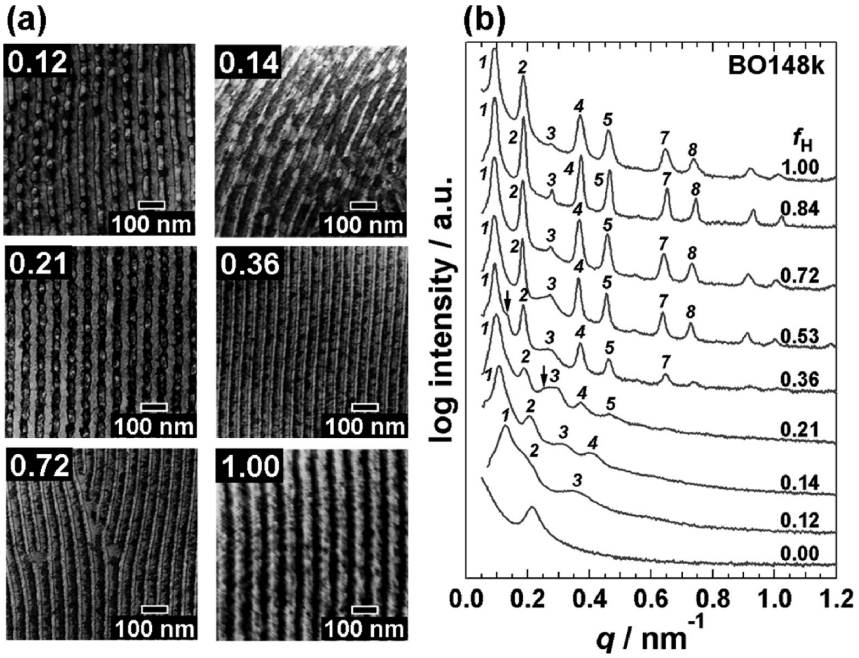

Figure 5. (a) TEM micrographs and (b) SAXS profiles of BO148k having various f_H values. The numbers at the upper left hand of each TEM micrograph represent f_H. Integer order numbers in SAXS profile indicate lamellar structures, while the arrows denote another structure.

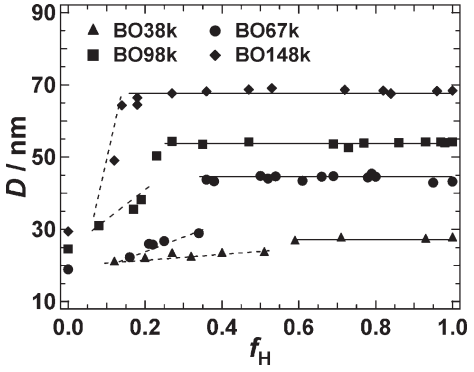

Figure 6. Changes in lamellar domain spacing, D, as a function of f_H for BO38k (▲), BO67k (●), BO98k (■), and BO148k (◆). Ds at $f_H = 0$ represent correlation length estimated from the peak top of the correlation hole peaks of nonhydrolyzed BOs. D increases as f_H increases (broken line) and remains constant (solid line) after reaching a specific f_H for all cases.

top of the correlation hole peaks of the nonhydrolyzed samples. It is apparent that D increases as f_H increases and shows an abrupt jump at a critical conversion rate, $f_{H,c}$, and remains constant onward. This means that the chains gradually deviate from a random coil conformation with increasing f_H and suddenly stretch perpendicular to the lamellar interface due to the increase in segregation power upon hydrolysis. However, the increase in D is relatively small for BO38k because of the small molecular weight. Furthermore, an increase of ca. 2.3-fold in D after full hydrolyzation is realized for all BOs, which will be discussed quantitatively later. Taking only polymer density into account, the ratio of D at $f_H = 1$ to that at $f_H = 0$ is merely 0.95, since bulk densities, ρ, for B, O, and H are 0.94, 1.00, and 1.16 g/cm^3, respectively. Therefore, the increase in χ parameter is dominantly responsible for the increment in D as hydrolysis reaction proceeds.

To elucidate the significance of $f_{H,c}$, degree of segregation at $f_{H,c}$, $\chi_c N$, was estimated and compared. Since the statistical behavior of the hydrolysis reaction is confirmed,[42] χ_c can be calculated based on the random copolymer theory,[43−45]

$$\chi_c = f_{H,c}\chi_{BH} + (1 - f_{H,c})\chi_{BO} - f_{H,c}(1 - f_{H,c})\chi_{OH} \quad (1)$$

where χ_{ij} is the interaction parameter between different components of i and j (i and j denote B, O, or H) approximated from solubility parameter, β, using eq 2.[46]

$$\chi_{ij} = \frac{v_0}{RT}(\beta_i - \beta_j)^2 \quad (2)$$

Here, v_0 is the average monomer volume ($=(v_i v_j)^{1/2}$), R is the gas constant, and T is the temperature. T_g of O component (=373 K) was substituted for T in eq 2 because O possesses the lowest T_g and the microphase-separated structures should be frozen at the temperature during cooling process. β was calculated from group contribution method, and the χ_{BH}, χ_{BO}, and χ_{OH} values obtained are 0.445, 0.003, and 0.386, respectively. N dependence of $f_{H,c}$ and $\chi_c N$ is shown in Figure 7. It is evident that $f_{H,c}$ decreases as N becomes larger; however, $\chi_c N$ is nearly constant for the whole range of N investigated. Besides that, $f_{H,c}N$ was found to be ca. 120 for all BOs. This indicates that the significant change in D at a specific f_H for each molecule with different molecular weight is associated with a transition in the aggregation state.

Figure 8 depicts the relationship between D/D_0 and χN for BO67k, BO98k, and BO148k where D/D_0 indicates the degree of chain stretching compared to its random coil state. Since the correlation hole peak of BO38k was hard to be detected, the D/D_0 of BO38k could not be evaluated precisely. D/D_0 values from three different BOs overlap each other within the whole range of

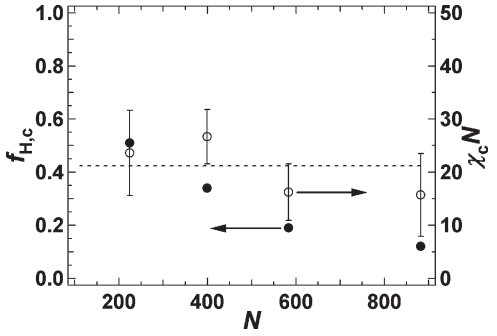

Figure 7. N dependence of the critical conversion rate, $f_{H,c}$ (filled symbols), and its degree of segregation, $\chi_c N$ (opened symbols), where χ is the interaction parameter and N is the degree of polymerization. Dotted line shows the average value of $\chi_c N$.

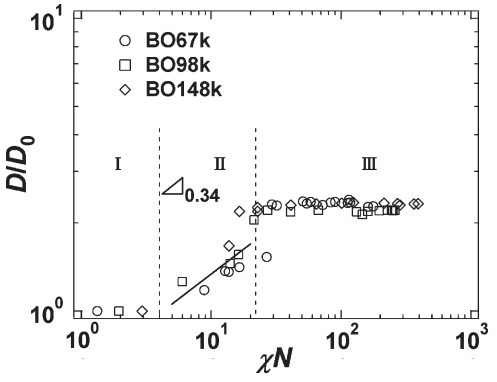

Figure 8. Relationship between D/D_0 and χN for BO67k (○), BO98k (□), and BO148k (◇). D_0 is the correlation length obtained from the nonhydrolyzed sample.

χN, signifying that the changes in D/D_0 for all hydrolyzed BOs are scaled by the segregation strength, χN. Three regimes can be distinguished in Figure 8: (I) $D/D_0 \sim 1$, (II) D/D_0 is proportional to $(\chi N)^{0.34}$, and (III) D/D_0 is constant to be 2.3. This means that the chains initially adopt Gaussian conformation in regime I and stretch gradually with increasing χN in regime II where they reach an equilibrium stretched state in regime III. Since the $\chi_c N$ is consistent with the boundary between regime II and regime III, the abrupt change in D shown in Figure 6 represents the transition from regimes II to III. It should be noted that the D/D_0 values are constant in two regimes of (I) and (III), reflecting that the structural similarity of chain conformations are maintained and the scaling laws can be applied in each regime. However, it is worth noting that the scaling law can only be applied in regime II in a strict sense of χN.

To determine the aggregation state in each regime, D was examined as a function of N. Figure 9a shows the double-logarithmic plot of D and N at $f_H = 0.00$ ($\chi = 0.003$) corresponding to regime I in Figure 8. D is proportional to $N^{0.55}$, meaning that BO chains obey nearly Gaussian statistics, and this regime is assigned to the weak segregation regime. This exponent ($\delta = 0.55$) is in reasonably good agreement with that of the reported values.[11−14] Figure 9d shows the relationship between D and N at $f_H = 1.00$, corresponding to regime III in Figure 8. Here, D is proportional to $N^{0.67}$, meaning that the chains are stretched and that a narrow interface is formed after full conversion of O into H. In addition, $D \sim N^{0.67\pm0.01}$ was also observed for f_H above 0.60 where all BOs have shown a sudden increase in D. On the basis of these results, it is obvious that regime III is the strong segregation regime.[15−20] The two exponents (δ = 0.55 and 0.67) directly reflect the extent of chain stretching perpendicular to the domain interfaces in these regimes.

Parts b and c of Figure 9 represent D vs N at $f_H = 0.12$ in regime II and at $f_H = 0.34$ which consumes Ds from regimes II and III, respectively. The scaling of $D \sim N^{\delta}$ cannot be simply applied to Ds in regime II because D/D_0 increases with χN (Figure 8). Nevertheless, if the relationship between D and N is analyzed ignoring the physical meaning, we obtained the scaling behavior of $D \sim N^{0.87}$ for $f_H = 0.12$ and $D \sim N^{0.81}$ for $f_H = 0.34$. Note that even combining Ds from regimes II and III in Figure 9c, the apparent scaling behavior was shown. Almdal et al. reported that the scaling behavior of $D \sim N^{0.80}$ was observed for poly(-(ethylene-*alt*-propylene)-*block*-polyethylene) (PEP−PEE) above and below the ODT.[24] Papadakis et al. also reported that the scaling behavior of $D \sim N^{0.83}$ was found around the crossover between the intermediate and strong segregation regimes for poly(styrene-*block*-butadiene) (SB).[25] These two reported data are consistent with our data shown in Figure 9b,c. Hence, it is obvious that regime II in Figure 8 corresponds to the intermediate segregation regime.[21−26] In a phenomenological sense, we admit that the D is proportional to $N^{0.80}$ in this regime. However, from the viewpoint of physical chemistry, there is no proper reason to think that this exponent indicates the chain dimension normal to the lamellar interface since the D/D_0 increases with increasing χN. Hence, we claim here that the intermediate segregation regime is defined again as the one in which the chain dimension cannot be discussed based on simple scaling analyses but in which the D/D_0 is proportional to $(\chi N)^{0.34}$.

Effect of Hydrogen Bonding on *D*. Another trend in the changes of D upon hydrolysis reaction is that it becomes constant after the abrupt increase although f_H keeps on increasing (see Figure 6). This result implies that the aggregation state in the SSL is unchanged regardless of the increase in χ. This seems to contradict the notion that D increases as the repulsive force becomes stronger. According to the SSL theory, by minimizing the free energy of forming microphase-separated structure from a block copolymer, D can be expressed by[16]

$$D = AN^{2/3}\chi^{1/6} \tag{3}$$

where A is a prefactor including the average segment length for component polymer, hydrolyzed BO in the present case. Here, we assume that A is constant throughout the hydrolysis reaction and treat it as a fitting parameter. The effect of hydrogen bonding was considered to represent χ because H is known to self-associate through hydrogen bonding. On the basis of hydrogen bonding polymer blends theory, free energy of mixing can be constructed by simply adding an external hydrogen bonding term, ΔG_H, to the conventional Flory−Huggins formula.[47] ΔG_H reflects the free energy change corresponding to the hydrogen bonding and basically affects the enthalpic part of the system, meaning χ. Hence, this concept was applied to formulate χ_{eff} for the present hydrolyzed BOs. It can be written as

$$\chi_{eff} = f_H\chi_{BH} + (1 - f_H)\chi_{BO} - f_H(1 - f_H)\chi_{OH} - p_H f_H \phi_H(\ln K) \tag{4}$$

where the sum of the first three terms is the non-hydrogen-bonding contribution similar to that of eq 1 and the last term is the

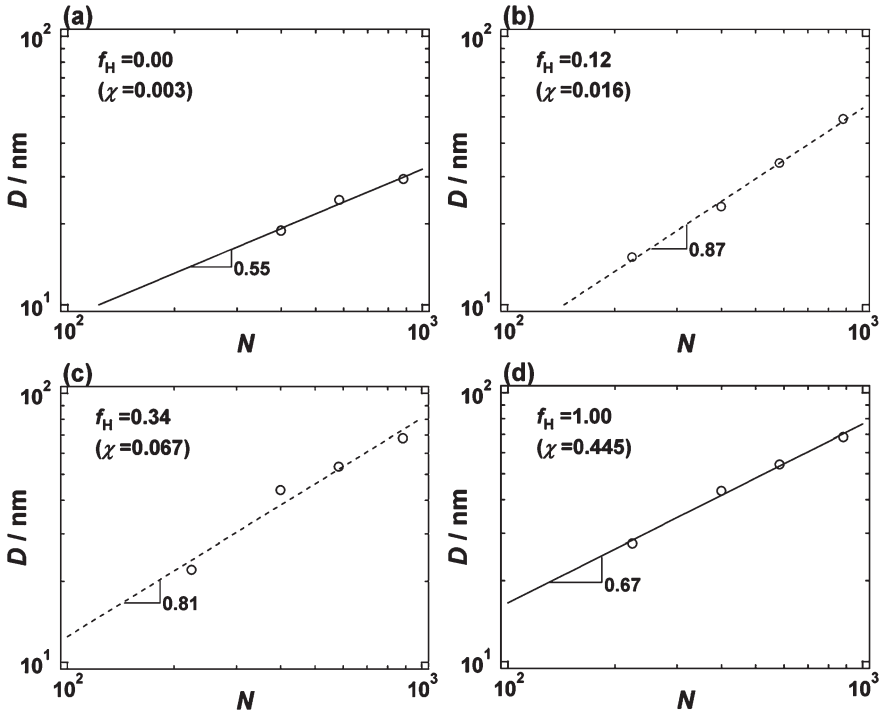

Figure 9. Relation between D and N at four different f_Hs on double-logarithmic scale ((a) 0.00, (b) 0.12, (c) 0.34, and (d) 1.00). Solid and broken lines are the least-squares approximated lines used to determine the δ for the scaling behavior of D with N, $D \sim N^{\delta}$.

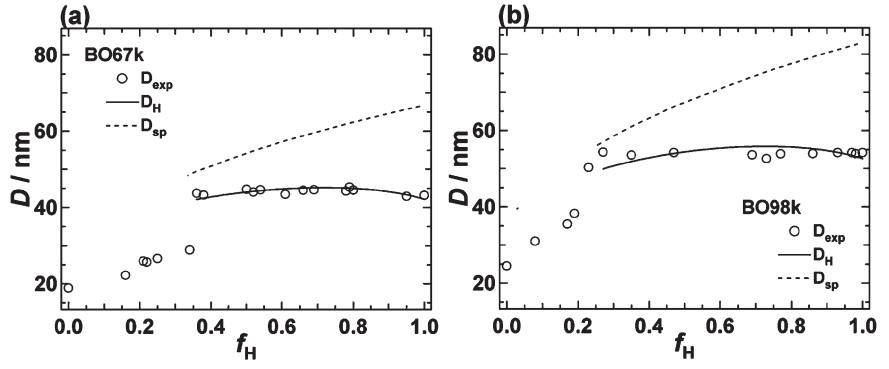

Figure 10. Comparison of D obtained from the study, D_{exp} (○), to that calculated from strong segregation limit theory using χ that was estimated with and without considering self-association of H, D_H (solid line) and D_{sp} (broken line), respectively, as a function of f_H. (a) is for BO67k and (b) represents BO98k. The prefactor A is 1.4.

dimensionless hydrogen-bonding term determined from

$$\Delta G_H = -RT \ln K \quad (5)$$

where K is equilibrium association constant of H. The K value for multimer formation of H component was already evaluated to be 66.8 by IR spectroscopy.[47b] The product $p_H f_H \phi_H$ denotes the fraction of hydrogen bonds where p_H is the probability of the formation of hydrogen bonds and ϕ_H is the volume fraction of H. Hence, in order to evaluate the effect of hydrogen bonding on D, the relationship between D and f_H was analyzed based on eqs 3 and 4 using A and p_H as fitting parameters.

Figure 10 shows Ds for BO67k and BO98k as a function f_H obtained from this study (D_{exp}) and those computed from SSL theory using well-established eq 3 based on eq 1 (D_{sp}, sp represents solubility parameter) and the modified one based on eq 4 (D_H). If A = 1.4 and p_H = 0.25 are used, the calculated D_H values which are drawn in solid lines in Figure 10a,b are in good agreement with D_{exp}s for both BO67k and BO98k. The same values of p_H for BO67k and BO98k might probably correspond to critical number of hydrogen bonds that related to $f_{H,c}N \sim 120$. On the other hand, if we assume no effect of hydrogen bonding (i.e., p_H = 0), D_{sp} increases with f_H for both BO67k and BO98k as expressed in broken lines. Therefore, self-association of H through hydrogen bonding compensates for the repulsive force among components resulting in constant D in the strong segregation region.

dx.doi.org/10.1021/ma102440a |*Macromolecules* 2011, 44, 2799–2807

CONCLUSIONS

Study on the morphologies of symmetric BO upon hydrolysis reaction was conducted by means of TEM and SAXS. An O/H mixed block is produced through the controlled hydrolysis reaction. Nonhydrolyzed samples showed no microphase-separated structure, whereas all hydrolyzed ones exhibited predominantly lamellar structures with a small portion of cylindrical one. This implies that the repulsive force against B block becomes stronger when O is converted into H. Lamellar domain spacing increased with f_H, where it abruptly increased at $f_{H,c}$, indicating chain stretching in a perpendicular direction to the lamellar interface as f_H increases and discontinuous change in the aggregation state at a specific χ. The normalized domain spacings, (D/D_0)s, were scaled by segregation strength, χN. Three regimes can be distinguished from the plot of D/D_0 vs χN: (I) the weak segregation regime with $D/D_0 \sim 1$ that associates with the scaling behavior of $D \sim N^{0.55}$, (II) the intermediate segregation regime with the scaling behavior of $D/D_0 \sim (\chi N)^{0.34}$, and (III) the strong segregation regime with $D/D_0 \sim 2.3$, which corresponds to $D \sim N^{0.67}$. The scaling behavior of $D \sim N^{0.80}$ in the intermediate segregation regime was observed in this study; however, this regime is redefined as the one in which the chain dimension cannot be discussed based on simple scaling analyses but in which the D/D_0 is proportional to $(\chi N)^{0.34}$. A computation of D based on SSL theory taking hydrogen bonding into account to the estimation of interaction parameter shows that hydrogen bonding from self-association of H compensates for the repulsive force among components which leads to a constant D after $f_{H,c}$.

AUTHOR INFORMATION

Corresponding Author

*E-mail yushu@apchem.nagoya-u.ac.jp, Tel +81-52-789-4604, Fax +81-52-789-3210.

ACKNOWLEDGMENT

This research was in part supported by the Grant-in-Aids for Scientific Research (A) (No. 22245038), for Young Scientists (A) (No. 22685013), the Priority Area "Soft Matter Physics" (No. 863), the Global COE program "Elucidation and Design of Materials and Molecular Functions" from the Ministry of Education, Culture, Sports, Science, and Technology (MEXT), Japan, and the aid fund for doctoral students' research of Nagoya University, Japan. This work was performed using BL-15A of Photon Factory, Institute of Materials Structure Science, High Energy Accelerator Research Organization, Japan under the program number of 2008G701. The authors acknowledge the Division for Medical Research Engineering, Nagoya University Graduate School of Medicine, for technical support of TEM observation.

REFERENCES

(1) Chan, V. Z. H.; Hoffman, J.; Lee, V. Y.; Iatrou, H.; Avgeropoulos, A.; Hadjichristidis, N.; Miller, R. D.; Thomas, E. L. *Science* **1999**, *286*, 1716–1719.

(2) (a) Mao, H. M.; Hillmyer, M. A. *Macromolecules* **2005**, *38*, 4038–4039. (b) Kubo, T.; Wang, R. F.; Olson, D. A.; Rodwogin, M.; Hillmyer, M. A.; Leighton, C. *Appl. Phys. Lett.* **2008**, *93*, 13112.

(3) (a) Li, L.; Yokoyama, H.; Nemoto, T.; Sugiyama, K. *Adv. Mater.* **2004**, *16*, 1226–1229. (b) Yokoyama, H.; Li, L.; Nemoto, T.; Sugiyama, K. *Adv. Mater.* **2004**, *16*, 1542–1546.

(4) Uehara, H.; Yoshida, T.; Kakiage, M.; Yamanobe, T.; Komoto, T.; Nomura, K.; Nakajima, K.; Matsuda, M. *Macromolecules* **2006**, *39*, 3971–3974.

(5) Kamperman, M.; Garcia, C. B. W.; Du, P.; Ow, H. S.; Wisner, U. *J. Am. Chem. Soc.* **2004**, *126*, 14708–14709.

(6) (a) Komura, M.; Iyoda, T. *Macromolecules* **2007**, *40*, 4106–4108. (b) Watanabe, R.; Kamata, K.; Iyoda, T. *J. Mater. Chem.* **2008**, *18*, 5482–5491.

(7) Balazs, A. C.; Emrick, T.; Russell, T. P. *Science* **2006**, *314*, 1107–1110.

(8) Lin, Y.; Boker, A.; He, J.; Sill, K.; Xiang, H.; Abetz, C.; Li, X.; Wang, J.; Emrick, T.; Long, S.; Wang, Q.; Balazs, A. C.; Russell, T. P. *Nature* **2005**, *434*, 55–59.

(9) Cho, B. K.; Jain, A.; Gruner, S. M.; Wiesner, U. *Science* **2004**, *305* 1598–1601.

(10) Watkins, P. K.; Walker, A. B.; Verschoor, G. L. B. *Nano Lett.* **2005**, *5*, 1814–1818.

(11) Leibler, L. *Macromolecules* **1980**, *13*, 1602–1617.

(12) Mayes, A. M.; de la Cruz, M. O. *Macromolecules* **1991**, *24*, 3974–3976.

(13) Owens, J. N.; Gancarz, I. S.; Korberstein, J. T.; Russell, T. P. *Macromolecules* **1989**, *22*, 3380–3387.

(14) Wolff, T.; Burger, C.; Ruland, W. *Macromolecules* **1994**, *27*, 3301–3309.

(15) (a) Helfand, E. *Macromolecules* **1975**, *8*, 552–556. (b) Helfand, E.; Wasserman, Z. R. *Macromolecules* **1976**, *9*, 879–888.

(16) Semenov, A. N. *Sov. Phys. JETP* **1985**, *61*, 733.

(17) (a) Ohta, T.; Kawasaki, K. *Macromolecules* **1986**, *19*, 2621–2623. (b) Kawasaki, K.; Kawakatsu, T. *Macromolecules* **1990**, *23*, 4006–4019. (c) Honda, T.; Kawakatsu, T. *J. Chem. Phys.* **2008**, *129*, 114904.

(18) DiMarzio, E. A. *Macromolecules* **1988**, *21*, 2261–2269.

(19) (a) Hahimoto, T.; Todo, A.; Itoi, H.; Kawai, H. *Macromolecules* **1977**, *10*, 377–384. (b) Hashimoto, T.; Shibayama, M.; Kawai, H. *Macromolecules* **1980**, *13*, 1237–1247. (c) Hashimoto, T.; Fujimura, M.; Kawai, H. *Macromolecules* **1980**, *13*, 1660–1669.

(20) (a) Matsushita, Y.; Mori, K.; Saguchi, R.; Nakao, Y.; Noda, I.; Nagasawa, M. *Macromolecules* **1990**, *23*, 4313–4316. (b) Matsushita, Y.; Mori, K.; Mogi, Y.; Saguchi, R.; Noda, I.; Nagasawa, M.; Chang, T.; Glinka, C. J.; Han, C. C. *Macromolecules* **1990**, *23*, 4317–4321.

(21) (a) Melenkevitz, J.; Muthukumar, M. *Macromolecules* **1991**, *24*, 4119–4205. (b) Lescanec, R. L.; Muthukumar, M. *Macromolecules* **1993**, *26*, 3908–3916. (c) Muthukumar, M. *Macromolecules* **1993**, *26*, 5259–5261.

(22) Barrat, J. L.; Fredrickson, G. H. *J. Chem. Phys.* **1991**, *95*, 1281–1289.

(23) Tang, H.; Freed, K. F. *J. Chem. Phys.* **1992**, *96*, 8621–8623.

(24) (a) Almdal, K.; Rosedale, J. H.; Bates, F. S.; Wignall, G. D.; Fredrickson, G. H. *Phys. Rev. Lett.* **1990**, *65*, 1112–1115. (b) Rosedale, J. H.; Bates, F. S.; Almdal, K.; Mortensen, K.; Wignall, G. D. *Macromolecules* **1995**, *28*, 1429–1443.

(25) Papadakis, C. M.; Almdal, K.; Mortensen, K.; Posselt, D. *Europhys. Lett.* **1996**, *36*, 289–294.

(26) Winey, K. I.; Gobran, D. A.; Xu, Z.; Fetters, L. J.; Thomas, E. L. *Macromolecules* **1994**, *27*, 2392–2397.

(27) Lodge, T. P.; Pan, C.; Jin, X.; Liu, Z.; Zhao, J.; Maurer, W. W.; Bates, F. S. *J. Polym. Sci., Part B: Polym. Phys.* **1995**, *33*, 2289–2293.

(28) Quinn, J. D.; Register, R. A. *J. Polym. Sci., Part B: Polym. Phys.* **2009**, *47*, 2106–2113.

(29) Budhlall, B. M.; Landfester, K.; Sudol, E. D.; Dimonie, V. L.; Klein, A.; El-Aasser, M. S. *Macromolecules* **2003**, *36*, 9477–9484.

(30) Halverson, F.; Lancaster, J. E.; O'Connor, M. N. *Macromolecules* **1985**, *18*, 1139–1144.

(31) Merle, L.; Merle, Y. *Macromolecules* **1982**, *5*, 360–366.

(32) Adams, J. L.; Quiram, D. J.; Graessley, W. W.; Register, R. A.; Marchand, G. R. *Macromolecules* **1998**, *31*, 201–204.

(33) Hahn, S. F. *J. Polym. Sci., Part A: Polym. Chem.* **1992**, *30*, 397–408.

(34) Gehlsen, M. D.; Bates, F. S. *Macromolecules* **1993**, *26*, 4122–4127.

(35) Xu, K.; Li, K.; Khanchaitit, P.; Wang, Q. *Chem. Mater.* **2007**, *19*, 5937–5945.

(36) Mokrini, A.; Acosta, J. L. *Polymer* **2001**, *42*, 9–15.
(37) (a) Zhang, W.; Dubois, M.; Guerin, K.; Hamwi, A. *Polymer* **2007**, *48*, 3961–3973. (b) Dubois, M.; Guerin, K.; Giraudet, J.; Pilichowski, J. F.; Thomas, P.; Delbe, K.; Mansot, J. L.; Hamwi, A. *Polymer* **2005**, *46*, 6736–6745.
(38) (a) Davidock, D. A.; Hillmyer, M. A.; Lodge, T. P. *Macromolecules* **2004**, *37*, 397–407. (b) Reisinger, J. J.; Hillmyer, M. A. *Prog. Polym. Sci.* **2002**, *27*, 971–1005. (c) Ren, Y.; Lodge, T. P.; Hillmyer, M. A. *Macromolecules* **2000**, *33*, 866–876.
(39) Park, M. J.; Balsara, N. P. *Macromolecules* **2008**, *41*, 3678–3687.
(40) Kimishima, K.; Jinnai, H.; Hashimoto, T. *Macromolecules* **1999**, *32*, 2585–2596.
(41) Kawaguchi, D.; Nomura, H.; Rahman, S. S. A.; Nakayama, M.; Matsushita, Y. *Macromolecules* **2009**, *42*, 8992–8997.
(42) Rahman, S. S. A.; Kawaguchi, D.; Matsushita, Y. *Polymer* **2011**, *52*, 164–171.
(43) Paul, D. R.; Barlow, J. W. *Polymer* **1984**, *25*, 487–494.
(44) Kambour, R. P.; Bendler, J. T.; Bopp, R. C. *Macromolecules* **1983**, *16*, 753–757.
(45) ten Brinke, G.; Karasz, F. E.; MacKnight, W. J. *Macromolecules* **1983**, *16*, 1827–1832.
(46) Krause, S. In *Polymer Blends*; Paul, D. R., Newman, S., Eds.; Academic Press: New York, 1978; Vol. 1, Chapter 2, p 45.
(47) (a) Coleman, M. M.; Painter, P. C. *Prog. Polym. Sci.* **1995**, *20*, 1–59. (b) Serman, C. J.; Xu, Y.; Paul, P. C.; Coleman, M. M. *Polymer* **1991**, *32*, 516–521. (c) Painter, P. C.; Park, Y.; Coleman, M. M. *Macromolecules* **1988**, *21*, 66–72.